DEPOSITION, DIAGENESIS AND RESERVOIR QUALITY OF SANDSTONE RESERVOIRS: A CASE STUDY IN THE CUU LONG BASIN, OFFSHORE VIETNAM

Son Nguyen Trung*

Petroleum Geoscience Program, Department of Geology, Faculty of Science,
Chulalongkorn University, Bangkok 10330, Thailand
*Corresponding author email: trungson2427@gmail.com

Abstract

The sandstone reservoirs are major reservoirs in siliciclastic worldwide. Therefore, a good understanding of the development of internal rock properties is extremely important, especially in terms porosity and permeability (indicate reservoir storage and flow capacity), which are in turn controlled by mineral compositions, rock textures, and diagenetic processes. This project studied the E and F formations in three wells in the Cuu Long Basin, with the aim of better defining controls on porosity and permeability (poroperm), not just in terms of depositional character, but also diagenetic overprints. Core samples were analyzed via thin section observations, scanning electron microscopy (SEM), X-Ray diffraction (XRD), Capillary Pressure (PC) and Helium Porosity-Permeability measurements, together with petrophysical evaluation.

The E formation was deposited in a fluvial-lacustrine environment that is characterized by claystone/shale interbedded with sandstone, with reduced depositional permeability in the finer-grained intervals. XRD and SEM indicate rock quality in the sandstone reservoirs was influenced by a variety of authigenic minerals, such as carbonate cements, quartz overgrowths, zeolites, and laumontite clays, all of which tend to reduce poroperm. The F formation was deposited in a higher energy setting. This was mostly a braided channel environment indicated by a blocky shape in the wireline across the sandy interval and typically good primary porosity and permeability. As in the F formation, the reservoir quality is strongly controlled by diagenetic evolution. Pore throats in the E and F sandstones are reduced in size by intense compaction and a combination of pore-filling minerals including; calcite cements, authigenic clays, and quartz overgrowths, leading to a negative relationship with poroperm. However, this negative relationship is not as clear in the
E formation.

Keywords: E and F formation, depositional environment, diagenetic process, petrography, porosity and permeability.

1. Introduction

This study discusses deposition, diagenesis and reservoir quality of sandstone reservoirs using a case study in the Cuu Long basin, offshore Vietnam (Figure 1). The aim of this study is to establish main factors that influence reservoir quality by creating a better understanding of controls in the development of poroperm and the diagenetic evolution of the E and F formations. The work is based on the integration of rock properties with petrographic analysis (thin section petrography, XRD analyses, scanning electron microscopy (SEM)), Capillary pressure (PC), and petrophysical evaluation. Results can provide information to better constrain the depositional environment and diagenetic processes in the study area.

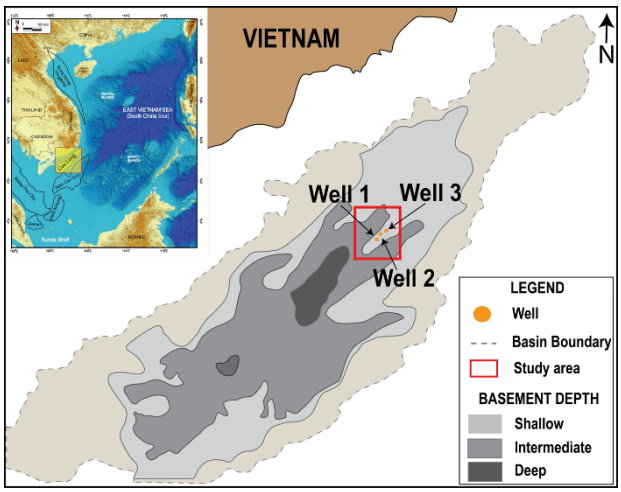

Figure 1: Overview of the study area. (Modified from Morley et al, 2019).

2. Geological setting

The Cuu Long Basin is a rift basin that experienced two main deformational events; 1) trans-tensional rifting from Eocene to mid-Early Oligocene (40-31Ma), followed by 2) transpression from Mid – Early Oligocene to Mid-late Oligocene (31-25Ma). This created three major tectonic styles namely: 1) rifting-related normal faulting from early Eocene to middle-Early Oligocene, 2) compression-related reverse faults and folds generated from middle-Early Oligocene to Mid-late Oligocene, and 3) thermal sagging from Mid-late Oligocene to the present, when the basin is fully filled by sediment without major faulting (Schmidt, 2019). The main fault systems trend NE-SW and NW-SE (Huy et al, 2012). Accommodation space in the Cuu Long Basin is filled completely with Tertiary sediments, with the Eocene F sequence being the oldest sedimentary unit in the basin, followed by Eocene-Oligocene E sequence, which included sequences C and D, and the Eocene succession, characterized by the Tra Cu and Ca Coi formation, which embraces sequences E and F (Dong and Hai, 2007). Sand E and F, which are the focus of this study, were deposited in the Early-Middle Eocene (F) and Late Eocene to Early-Oligocene (E) (Figure 2).

3. Methodology

For the first time, the results of several sets of analysis across three wells are integrated and combined in a multi-well synthesis. The aim is to better define controls on porosity and permeability not just in terms of depositional character, but also diagenetic overprints. Diagenetic intensity is estimated vertically and horizontally (between all wells) based on an integration of reservoir properties. Core photos, core analyses and the results of the petrographic study are integrated with helium-based porosity-permeability measurements from routine core analysis (RCA), well log analysis and capillary pressure (PC) measures. Thin sections, SEM Log shape and core data from all wells proved useful in defining various depositional environments in the study area. Depositional environments are cross-plotted against each other to better identify lithology variability and its tie to poroperm quality.

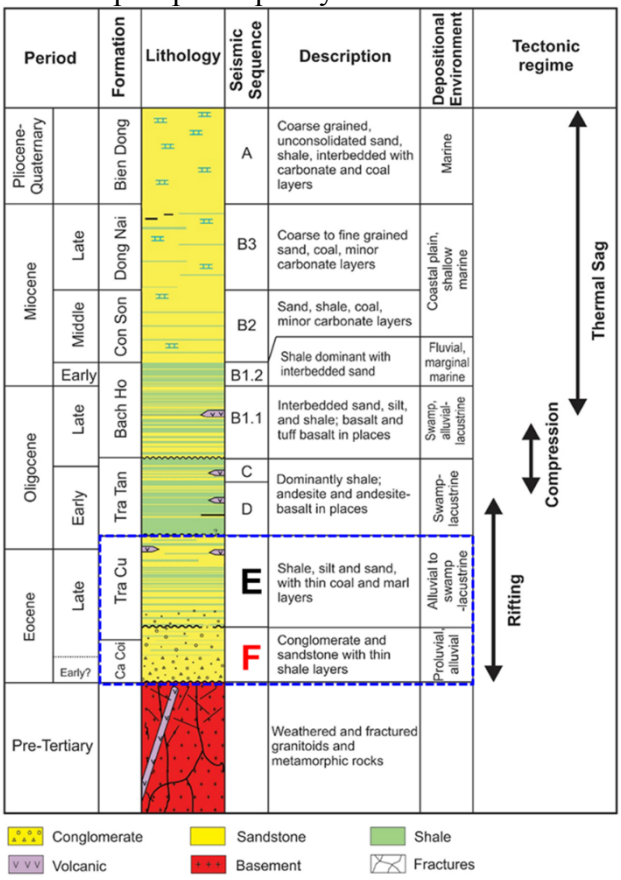

Figure 2. The stratigraphic column of the study area, focusing on the E and F formation as indicated by a blue rectangle (modified from W.J Schmitt, 2019).

4. Result

4.1 Core interpretation

Lacustrine shoreface/deltaic sandflat: Fine-grained sandstone is typical of this facies grouping. The primary structure is low angle bedding and indeterminate lamination (Figure.3).

Channel/Channel abandonment: These fining-upward sandy reservoir-quality units include mud rip-up clasts and some coarser grains at their bases that then pass up into cross-bedded units with muddy tops (Figure 4).

Overbank: These are very fine-grained sediments made up of mudstones and very fine siltstones that include some sandstone-filled burrows. There are some pyrite nodules and calcite-cemented mud clasts in several intervals (Figure 5).

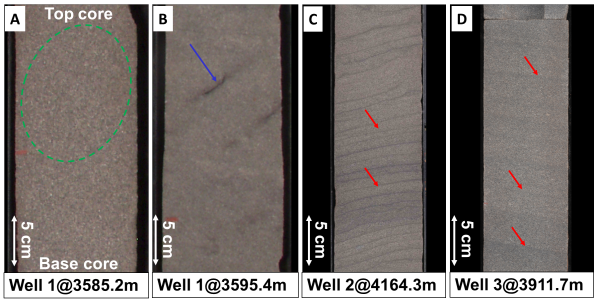

Figure 3. (A) Massive medium sandstone with a mottled texture (green arrow) indicating extensive bioturbation. (B) Fine sandstone including plant fragments (red arrow). (C) Low-angle lamination (red arrow) with fine-sand grain-size interlaminated with thin shales. (D) Indeterminate lamination (red arrow) with fine grain size.

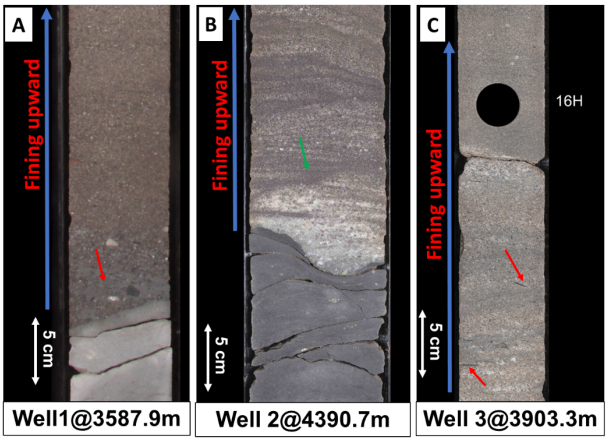

Figure 4. (A) Fining upward sandstones include very coarse grains and granules, mudstone clasts occur within some beds (red arrow). (B) Primary sedimentary structures are dominated by planar cross-bedding (green arrow) with fining-upward trends and erosional bases, exaggerated by compactional loading. (C) The fining-upward trend with the only fossil material observed within these facies being small plant fragments (red arrow).

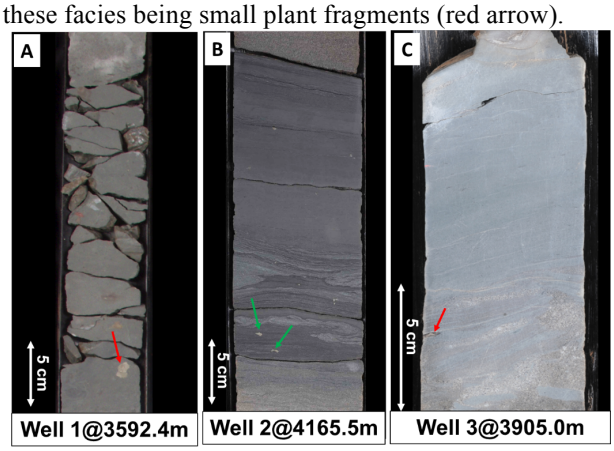

Figure 5. (A) Mudstones and very fine siltstones that include occasional nodular pyrite (arrow) and sand-filled burrows (at the top) in Well 1, (B) Mudstones and some nodular pyrite (arrow) in Well 2. (C) Very fine siltstone that includes a calcite-cement mud clast (arrow).

Braided fluvial: These sandstones range in grain size from very fine (lower) to coarse (middle). The thickness of individual beds ranges from about 10cm to 1.65m. The sandstones commonly include mud rip-up clasts, very coarse grains, granules and pebbles which are most common within bed bases (Figure 6).

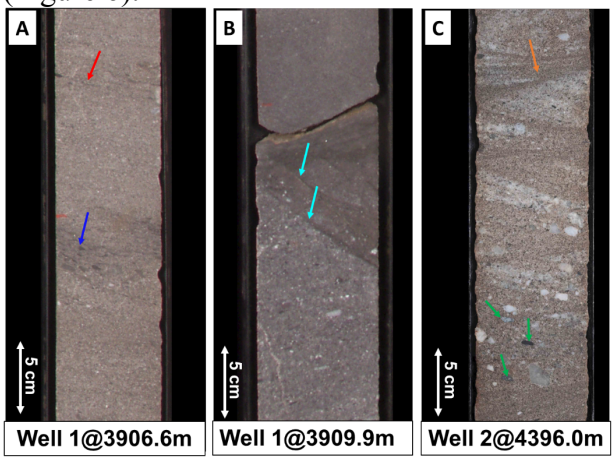

Figure 6. (**A**) The sandstones commonly include mud clast, very coarse grains, granules and pebbles (blue arrow). Fossil material includes some small plant fragments (red arrow). **(B)** A sequence of low-angle normal fractures at the contact between coarser and very fine sandstones. Fractures are clay smeared (aqua arrow). (**C**) The dominant primary sedimentary structure is planar cross-bedding which ranges in dip from horizontal to 45° (orange arrow). Some of the pebbles comprise green basement clasts, which are possibly basalt (green arrow).

Depositional Environment Interpretation

In general, the E sandstone has textural features and framework-grain compositions (lithic-arkoses and arkoses (Fig.9)) indicating that the sediment was transported over a distance that was not too far from its source, and that during deposition the sands were frequently subjected by periods of at least moderate current activity (sand deposition) alternating with periods of quiescence (clay deposition). This in combination with the palynology suggests that the sediments were deposited in a mostly lacustrine and fluvial environment.

Textural features and framework-grain compositions of the F sandstone indicates that the sediments were transported not too far from the source and that this sandstone was frequently subjected by high energy flows in a braided fluvial setting.

4.2 Petrophysical Analysis

Helium analytical results on core plugs from the E and F formation show a wide range of porosity and permeability, with porosity values from 2 to 16% (av.Φ =9.7%) and permeability values from 0.001 to 1000mD (av.K =30.8mD) in the E formation. The F formation generally shows higher porosity than the E formation, with porosity ranging from 2 to 18% (av. Φ =10.6%) and permeability ranging from 0.0001 to more 1000mD (av.K=66.7mD). Cross-plots of porosity and permeability show a good correlation between porosity and permeability in the both of E and F formations, with linear relationships

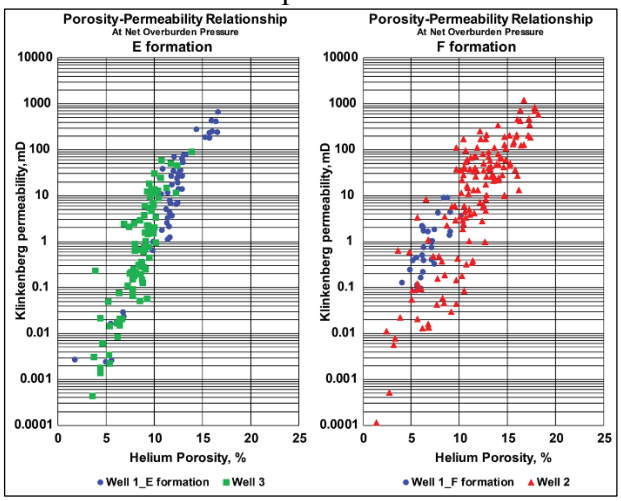

Figure 7. Cross-plots illustrating the relationship between porosity and permeability in the E and F formation.

The curvature of capillary pressure curves indicates the rock quality. The E formation and F formation examples that show more gentle curvatures related to reduced permeability, due to the impact of calcite cements in the sands. Poorer quality samples show high residual water saturation related to poorer sorting and finer grain sizes or poorer quality outputs can be related to calcite cements that have a negative relationship to poroperm characteristics**.** The analysis implies that there are relatively high porosity and permeability intervals within the overall lower porosity-permeability of dominant reservoirs.

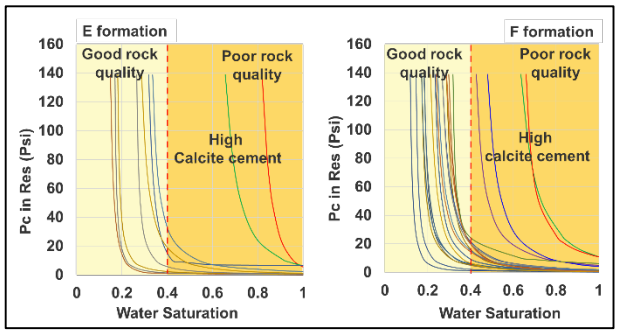

Figure 8. The curvature shape of the capillary pressure curve indicates the rock quality.

4.3 Petrographic Analysis

4.3.1 Sandstone detrital composition

Petrographic study shows the cored intervals in Well 1, Well 2 and Well 3. The R.L. Folk classification (1974) is used to classify sandstones with less than 15% detrital matrix. The Q; F; R components are Q = all quartz, except chert; F = feldspar + granitic fragments; R is all other rock fragments. Most of the samples are arkosic sandstones and lithic arkose sandstones (Figure 19).

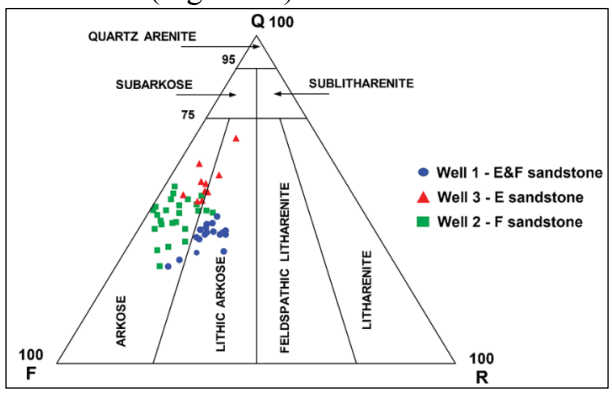

Figure 9. The detrital composition of samples with less than 15% detritals using R.L. Folk's classification (1974).

4.3.2 Visible porosity

Porosity in the E and F sandstones includes primary intergranular porosity (which is the space between grains) and secondary porosity which is mainly related to the dissolution of unstable detrital grains, such as volcanic fragments and feldspars (K-feldspar and plagioclase). The mechanical compaction of this cored interval is moderate, characterized by grain contacts that are mostly to point-to-point (blue arrow) some long-axis (green arrow) passing to occasional concavo-convex contacts (yellow arrow).

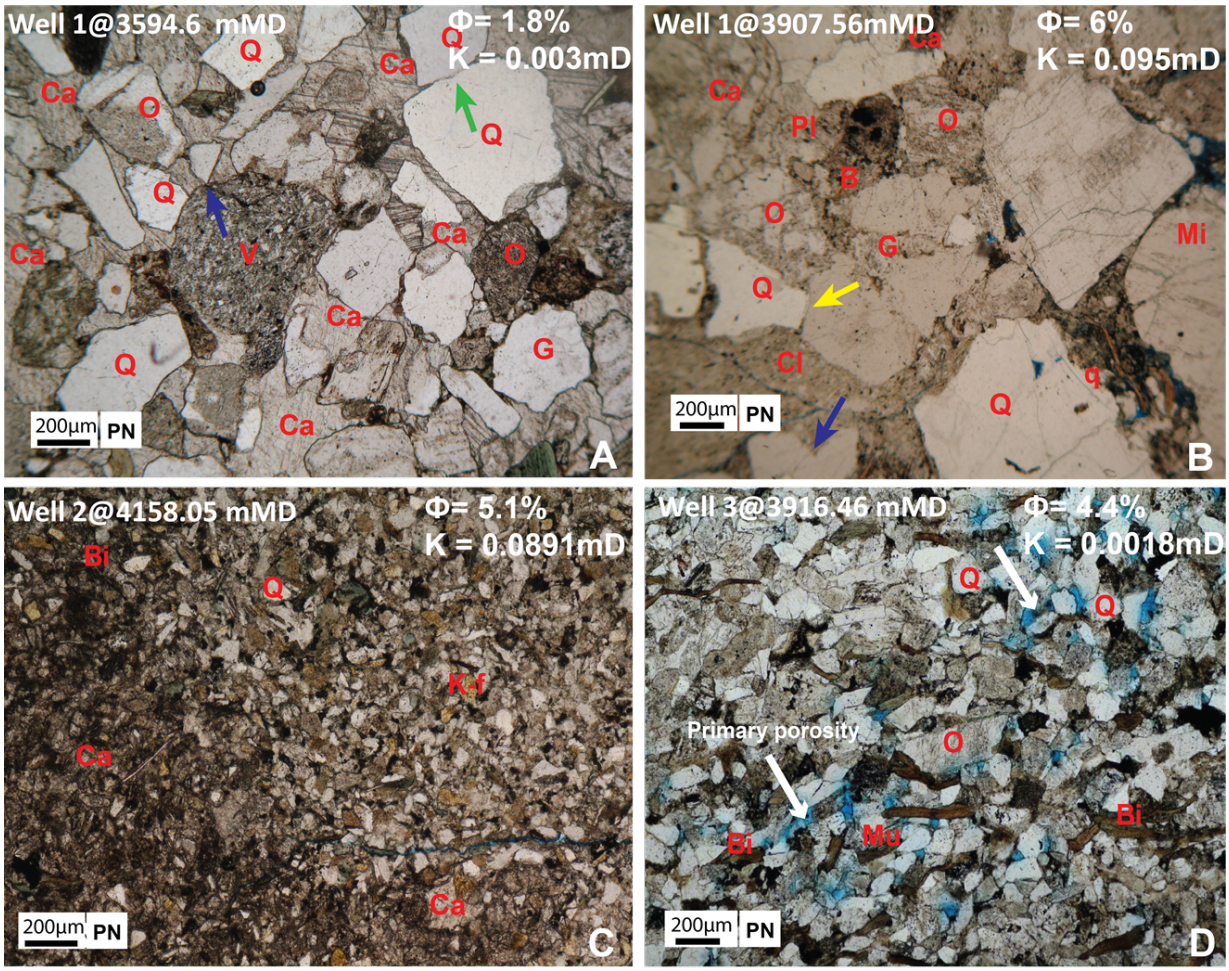

Figure 10. Thin section images of sandstones (Pore space is shown in blue, calcite cements (Ca), fill or partly fill intergranular pore spaces. (quartz (Q), quartz overgrowths (q), orthoclase (O), plagioclase (Pl), granitic (G), volcanic fragments biotite (Bi) and muscovite (Mu)).

4.3.3 Mineral framework grains

Whole-rock analysis (XRD) of samples in the cored intervals shows quartz dominates. Feldspars are the second most abundant component in the sandstones and consist of two types; potassium feldspar (K-F) and plagioclase. Petrography shows the dissolution of feldspar has generated secondary porosity, so enhancing total porosity.

Well 1_E sandstone, consists mainly of quartz (average 40%), K-feldspar and plagioclase (average 40%), clay minerals as mica, laumontite, kaolinite (average 18%) are present as are the carbonate minerals, calcite, dolomite, and siderite (average 2%)(Figure 11B). In comparison, XRD analysis of samples from in Well 3 (Figure 11D) has quartz averaging 29% and 38% in its K-F/plagioclase. This is lower than in Well 1, perhaps because the sedimentary source was different. The clay minerals contents in Well 3 are higher than in Well 1, perhaps because Well 3 was further from the sediment source than in Well 1, or it was deposited under lower overall energy conditions. Carbonate cement content in Well 3 (3%) is slightly higher than in Well 1 (2%).

Samples of Well 1 in the F sandstone consists of main quartz (average 54%), K-feldspar and plagioclase (average 34%), other clays such as mica, laumontite, kaolinite (average 18%) and the carbonate minerals, calcite, dolomite and siderite (average 1%) (Figure 12A). In comparison, the F sandstone in Well 2 has a quartz average of about 28% and 36% for K-feldspar /plagioclase content (Figure 12D). This is lower than in Well 1 as reflected in the petrographic typing of Well 1, which is mostly

lithic arkose with a lesser feldspar content than the arkoses the dominate in Well 2 (Figure 9).

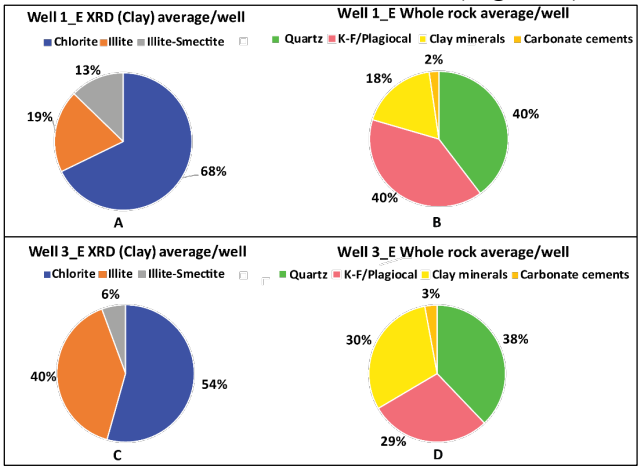

Figure 11. Illustrating the whole rock and XRD results in the E sandstones.

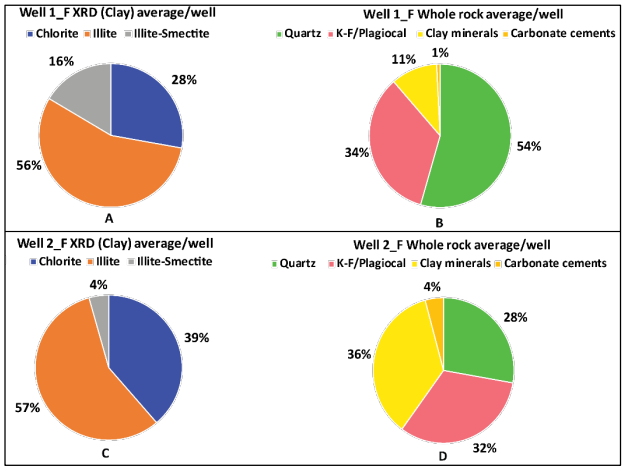

Figure 12. Illustrating the whole rock and XRD result in the F sandstones.

4.3.2 Authigenic Clays

The presence of clays in a sandstone across all wells tends to degrade reservoir quality.

Figure 13A illustrates authigenic chlorite aggregates (Ch) occur mostly as subhedral, thin plates that can fill pore spaces, together with illite (Il) and calcite. The macro/micropore sizes of < 20µm encompasses the remaining volumes of an occluded primary pore. A pore throat that is completely blocked by many large crystals of mosaic quartz overgrowth (q), leads to the initial pore throat is not only reduced in volume but also divided into very small pore channels (arrow) and so it becomes very tortuous (Figure 13B).

Figure 13C suggests the remaining intergranular pores (arrows) have now become isolated or retain very poor connectivity. In addition, authigenic illite aggregates (Il) fill intergranular pores and pore throats, illustrating how a small amount of authigenic illite can degrade so much the permeability.

Authigenic chlorite clay mineral occurs as thin, mats of crystals that coat detrital grains. Wispy and webby illite intermixed with platy chlorite can completely coat detrital grains and fill intergranular pores, resulting in a strongly reduced permeability (Figure 13D).

Detrital feldspar grains (F) can be dissolved and so form secondary pores. The orientation of the feldspar remnants suggests dissolution is crystallographically controlled. Locally, feldspar remnants are partly albitized and have been replaced with chlorite. This suggests that the dissolution of unstable detrital grains likely pre-dated chloritization in the paradiagenetic sequence (Figure 13E).

Figure 13F shows a blocky authigenic zeolite crystal (Z) that occupies intergranular pore space, so damaging the reservoir quality. A feldspar grain (F) has also been dissolved and albitized. Locally, authigenic clay minerals (Cl) occur as chlorite and illite/illite-smectite fills in secondary pores and can partly coat detrital grains. The strong development of quartz overgrowths (upper left) has also occluded pore throats.

Laumontite (a zeolite mineral) can replace feldspar as double-edge crystal grains or cleavage crack fills. Some pore-filling laumontites, as well as quartz overgrowths, can slow or inhibit further compaction (Figure 13C).

A negative relationship between total clay minerals and poroperm suggest the clay minerals are strongly degrading the porosity and permeability (Figure 14, 15). Pore-lining chlorite is directly precipitated on surfaces of grains, so extending into pore space, leading to a significant decrease in permeability (Figure 13A). Illite occurs as pore-linings and is partly pore filling and partly grain coating. It forms

irregular flakes with lath-like projections that can bridge intergranular spaces, so decreasing permeability and pore throat diameters (Figure 13B, 13D). Smectite/illite transforms into illite at higher temperatures and rarely occurs in the temperature ranges of most petroleum fields unless the reservoir is flushed by hydrothermal waters.

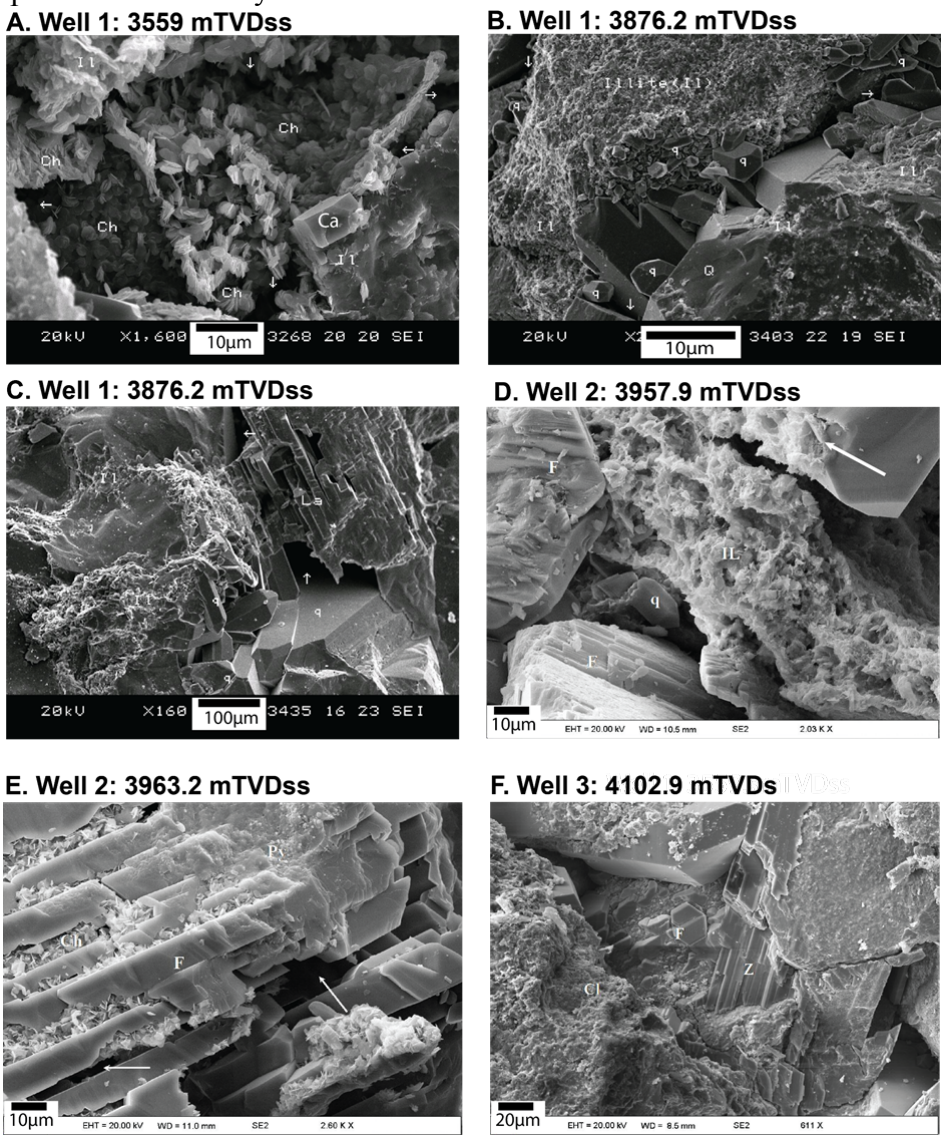

Figure 13. Scanning Electron Microscopy (SEM) of samples from all wells in the study area.

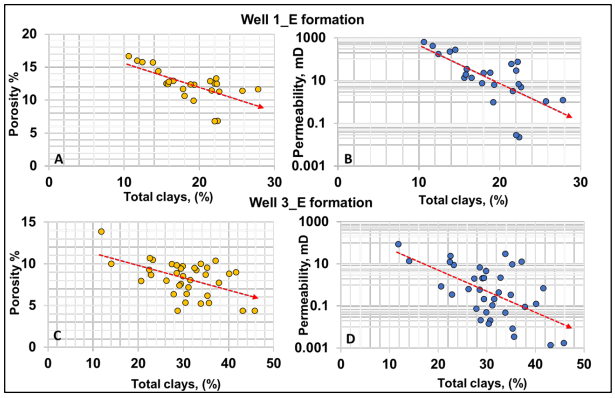

Figure 14. The relationship between permeability and total clays showing a negative trend in the E formation.

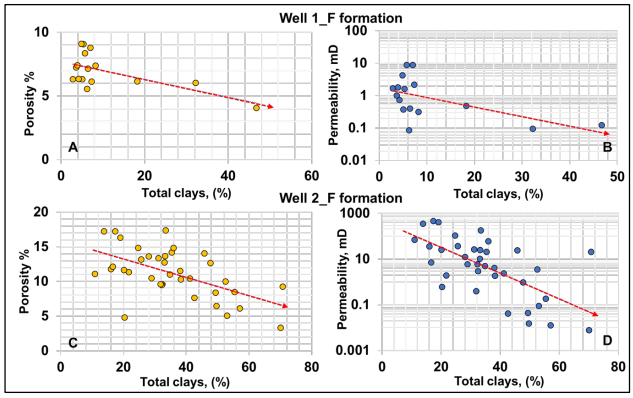

Figure 15. The relationship between permeability and total clay showing a negative trend in the F formation.

4.3.4 Quartz, Carbonate Cements

Carbonate cements in the study area are composed of calcite, with minor dolomite and siderite. Carbonate cements are observed in all wells and it is a significant factor influencing the poroperm quality of the studied sandstones. Figure 16A shows the abundance of carbonate cements is less than a certain threshold (about 10%) and illustrating the different amounts between the wells. The proportion of carbonate cements increases up to 32% in E formation of Well 1 (Well_E) and 20% in Well 2 (Figure 16A) with an average of 3% of rock volume in both wells. Carbonate cements in Well 3 and Well 1_F are less, with an average 1.3% and 2.6%, respectively. Figure 17 is a cross-plot with a carbonate cement value threshold of 1% or 2%, values less than this show an unclear relationship between carbonate cement and poroperm. However, when the proportion of calcite cements is higher than 1% (Well 1_E, Well 2, Well 3) or 2% (Well 1_F), there is a decrease of porosity and permeability with increasing carbonate cement content (Figure 17).

Quartz overgrowth cements, which are more abundant than carbonate cements, range from 4 % to 10%, average 7.4% in the E formation of Well 1, and mostly 3%-6% (average 3.9%) in the Well 3, and 2.7% in the Well 2, which also contains the highest levels of overgrowths from 4%-15% (average 11.8%). The formation of quartz (overgrowth) cement is an ongoing diagenetic process. It begins as one of the earlier burial phases when it can be covered by chlorite rims and can proceed until it fully fills primary pores (Figure 16B). Later quartz overgrowth cement generations develop over authigenic illite and present as pyramidal quartz and euhedral quartz crystals that partly fill primary porosity (Figure 13B, C, D).

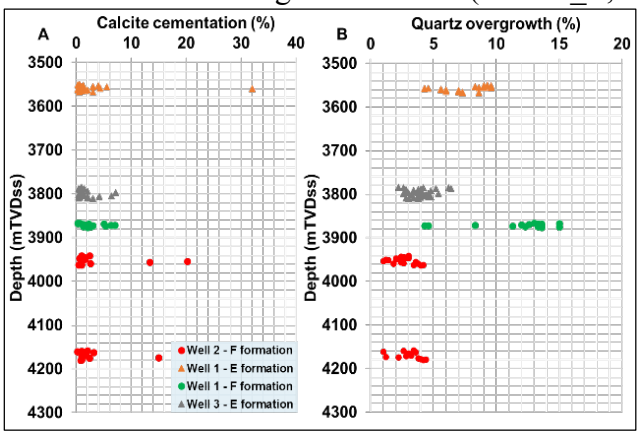

Figure 16. The proportion of carbonate cements and quartz overgrowth distribution.

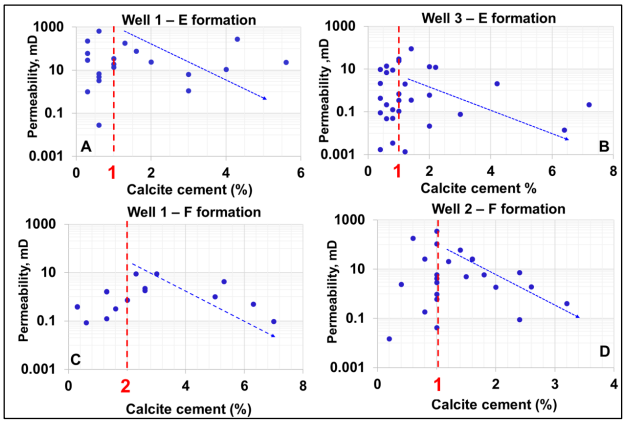

Figure 17. The relationship between permeability and calcite cements shows a negative trend.

5. Discussion

5.1 Key geological factors influencing on Porosity permeability in sandstone reservoir

5.1.1 Depositional environment

Based on the preceding observations, the lacustrine/deltaic-sandflat, channel, braided channel, and overbank deposits show significant differences in porosity and permeability. The overbank succession shows the lowest values (approximately av. Φ =5.9%, av K= 0.1mD), moderately higher values are observed in the channel and braided channel facies (about av.Φ = 9.7%, av.K = 28.8 mD and av.Φ = 9.5%, av.K= 34.9%, respectively) and the highest measured values occur in lacustrine shoreface/deltaic-sandflat facies. There is a good correlation of porosity and permeability in cross-plots of these facies (Figure 19). Well 3 and Well 2 show lower porosity and low permeability (Φ = 10%, K = 0.1mD) spreads in several samples (indicated by orange box) from the otherwise good quality lacustrine/deltaic sandflat facies (Figure 19A). In addition, the average porosity of Well 3 (av.Φ = 8.4%) is lower than Well 1 and Well 2 (av. 12.7% and 13.3%, respectively) in these facies. Similarly, a few samples from the channel facies in Well 1 and Well 2 illustrate low porosity and permeability (orange box) (Figure 19B). Almost all samples of overbank show low porosity and permeability, due to very fine to fine grain sizes (Figure 19C). The braided channel samples show significant differences between Well 1 and Well 2. The porosity of Well 2 is higher than Well 1 (approximately 10.9% and 7%, respectively) (Figure 19D). The differences in poroperm quality between the four facies reflect differences grain-size ranges in the same depositional setting and the variable influence of diagenetic alteration.

5.1.2 Compaction process

Compaction can be illustrated through plots between porosity and permeability with depth. All show an inverse relationship, with porosity decreasing in a particular formation with depth (Figure 20A and 20B). However, Well 1_F is less porous than the F sandstone in the upper part of well 2 because cementation is locally strong, especially the development of quartz (overgrowth) cement (from 11% up to 15% (Figure 16B)). Petrography shows quartz is widespread as large, euhedral and syntaxial overgrowth crystals (up to 10s and 100s μm in length), which can completely fill the remaining intergranular pores and so block pore throats in the Well 1_F.

5.1.3 Diagenetic process

Based on the above investigations and burial-history locations, the main digenetic events observed in E and F sandstone are summarized in Figure 21.

Some parts of the E and F sandstones show more advanced diagenetic textures such as; moderate compaction, strong development of quartz and albite overgrowths, pore-filling zeolites and calcite cements. Furthermore, the dissolution of unstable detrital grains and their conversion to more stable phases are also quite common. For instance, feldspar grains are partly dissolved or replaced by laumontite, zeolite and/or calcite. This suggests that the sandstone has been transformed in hydrothermal crossflows at moderate burial depths. Cements and authigenic minerals consist mainly of quartz overgrowths (commonly 7-9% in E formation and 11%-15% in F formation), zeolites (5-8% and 5-10%, respectively) with small amounts of calcite and authigenic clays. Zeolite and calcite often form as patches enclosing closely-packed detrital grains or fills in isolated intergranular pores. Remnant primary porosity was protected by the development of quartz and albite overgrowths. Grain contacts are mainly long and concavo-convex types, which tend to minimize the dimensions of pore throats.

5.2 Comparison of diagenesis between the study area and a nearby area

The study area is located near block 15-2 where a study was conducted on the E formation (Phuong, et al., 2017). Their work concluded that the main factors influencing rock quality were; compaction, cementation, and dissolution of unstable grains. My work concludes that the porosity and permeability in the studied wells are controlled by depositional

setting variably overprinted by cementation and mechanical compaction. Authigenic clay minerals as pore-linings or in grain-surrounding coats have destructive effects on porosity and permeability. The destructive effects of increasing clay content are similar in both areas (Figure 22 A-D vs. E-F).

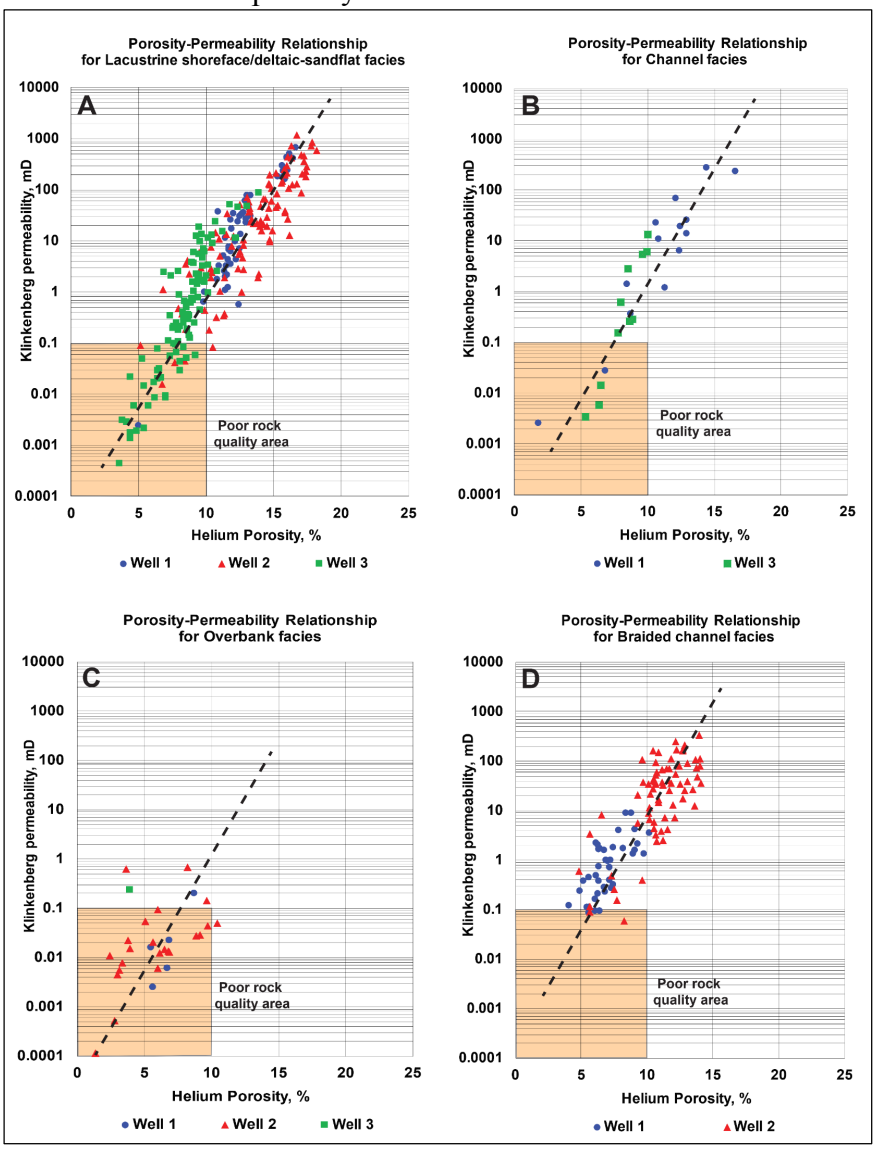

Figure 18. The poroperm relationship illustrates significant trends between facies.

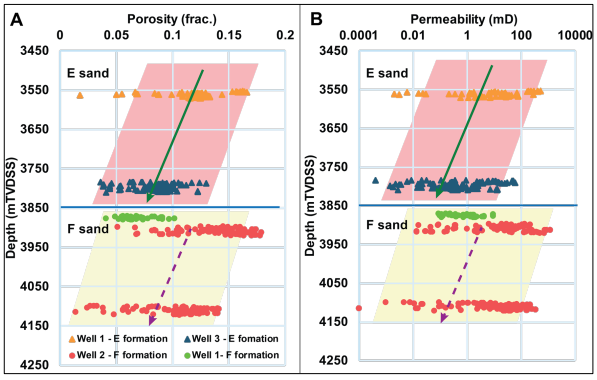

Figure 19. Core porosity (A) and core permeability (B) vs. true vertical depth subsea cross plots.

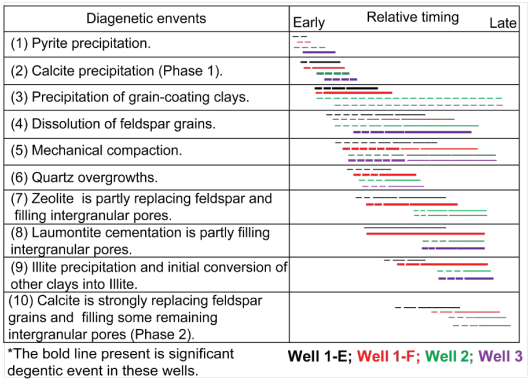

Figure 20. Paragenetic sequences across all wells.

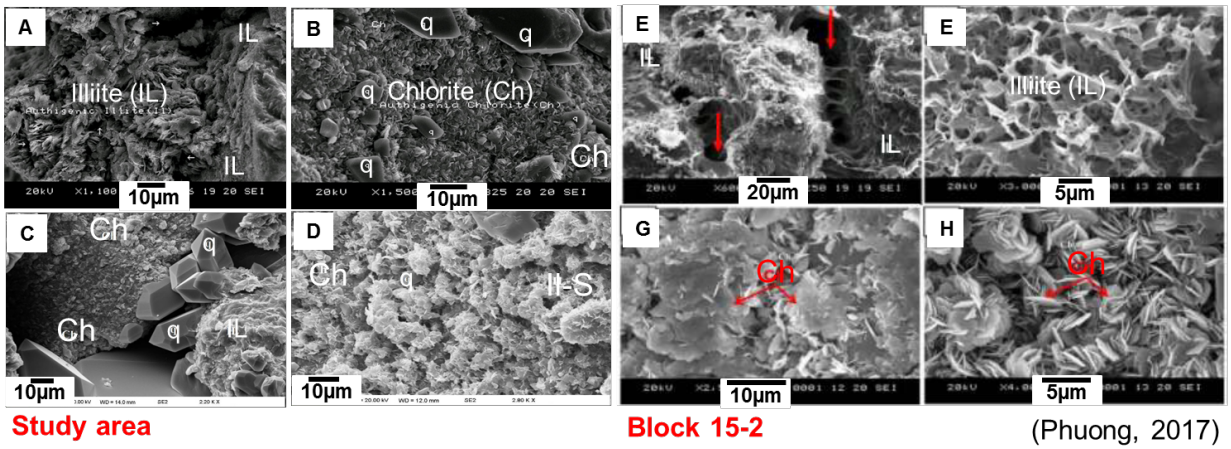

Figure 21. Morphologies of clay minerals in the E Formation in the study area compare to sediments in Block 15-2, Cuu Long basin.

6. Conclusions

The quality of reservoir sands in the study area is evaluated by integrating all petrography, XRD, RCA, SCAL, and conventional well-log data sets. The results quantify variations in the internal properties of the sandstone reservoirs. Based on the results of this study, the conclusions are:

1. There are four core-defined depositional facies, namely; 1) Lacustrine shoreface/deltaic sandflat (channel abandonment) sands which entrain numerous mud layers. 2) Channel sands which are generally indicated by fining-upward, bell shapes in GR and are mostly found in the E formation. 3) Braided channel sands are characterized by poorer sorting with mostly blocky shapes in GR, and is most abundant in the F formation. 4) The overbank succession shows the lowest poroperm values. Moderately higher poroperm values are observed in the channel and braided channel facies and the highest poroperm values tend to occur in lacustrine shoreface/deltaic-sandflat (channel abandonment) facies.

2. Rock property measures across the E and F formations show porosity and permeability ranges from low to high values of porosity and permeability. Generally, there is a tie to the depositional setting. But in intervals that are more subject to diagenesis and hydrothermal fluid crossflows, the enhanced formation of authigenic cements can degrade what were good quality sands at the time of deposition.

3. The curvature shape of capillary pressure curves indicates the rock quality. Some samples show a gentle curvature that relates to reduced permeability, poorer sorting, finer grain sizes and the impact of calcite cements.

5. Thin section study shows rock quality was largely controlled by a combination of mechanical and chemical compaction, as shown by grain contacts ranging from, point-to-point, to long-axis rotation, and concavo-convex styles being present in all three wells.

6. The negative relationship between total clay minerals and poroperm suggest the clay minerals reduce porosity and permeability. Pore-lining chlorite is directly precipitated on to detrital surfaces of grains and extends into pore space, leading to decreasing permeability. Authigenic illite also decreases permeability by blocking pore throats.

7. Chlorite is more abundant in the E sandstone than in the F sandstone. Chlorite tends to develop in sandstones richer in volcanic fragments. By contrast, illite is present in the F sandstone at much higher levels than in the E, so illite is likely a weathering product, but diagenetic illite is also created by reactions of smectite with pore fluids during deep burial.

8. Calcite cements can fill pores, reducing permeability and porosity in all wells. It can show a patchy or uneven distribution and was mostly generated in early diagenesis.

9. Compaction is illustrated in plots of porosity and permeability with depth. These plots show an inverse relationship with poroperm decreasing with depth.

10. The E and F sandstones have experienced a complex diagenetic evolution, as follows; (1) (2) pyrite and calcite precipitation, (3) precipitation of grain-coating clays, (4) dissolution of feldspar grains, (5) mechanical compaction (6) quartz overgrowths, (7) zeolites partly replacing feldspars, (8) laumontite cementation, (9) illite precipitation, (10) calcite strongly replacing feldspar grains.

11. A comparison with a result from a nearby area shows the depositional rock quality of E formation in that area was similarly influenced by diagenetic processes, such as compaction, cementation, and dissolution. The study in the adjacent area concluded that porosity and permeability were greatly impacted by formation authigenic clays, such as chlorite or illite, as wells as mechanical compaction.

7. Acknowledgements

I am very grateful to my supervisor, Prof. John Keith Warren. He continually and convincingly conveyed a spirit of challenge throughout my research at Chulalongkorn University

I also would like to thank Exploration and Production Centre (EPC), Vietnam Petroleum Institute (VPI) and the Vietnam National Oil and Gas Group (PVN) for providing the dataset for this research.

8. References

Chen, J., J. Yao, Z. Mao, Q. Li, A. Luo, X. Deng, and X. Shao, 2019, Sedimentary and diagenetic controls on reservoir quality of low-porosity and low-permeability sandstone reservoirs in Chang101, Upper Triassic Yanchang Formation in the Shanbei area, Ordos Basin, China: Marine and Petroleum Geology, v. 105, p. 204-221.

Dong, T, L., P. D. Hai, 2007. Cuu Long sedimentary basin and petroleum resources. The Petroleum Geology and Resources of Vietnam. In: The Science and Technology Publishing House, 1st ed.

Djebbar, T., C. D. Erle, 2015, Petrophysics: Theory and Practice of Measuring Reservoir Rock and Fluid Transport Properties, Gulf Professional Publishing, 894p.

Haile, B. G., T. G. Klausen, U. Czarniecka, K. Xi, J. Jahren, and H. Hellevang, 2018, How are diagenesis and reservoir quality linked to depositional facies? A deltaic succession, Edgeøya, Svalbard: Marine and Petroleum Geology, v. 92, p. 519-546.

Huy, N. X., Bae Wisup., T. N. San., V.T. Xuan., J. SungMin., Kim D.Y., 2012, Fractured basement reservoir and oil displacement mechanism in White Tiger Field, Offshore Vietnam. AAPG Search and Discovery Article, AAPG International Conference & Exhibition, Singapore, 16-19 September 2012.

Morley, R. J., V. D. Bui, T. T. Nguyen, A. J. Kullman, R. T. Bird, V. K. Nguyen, and H. C. Nguyen, 2019, High-resolution Palaeogene sequence stratigraphic framework for the Cuu Long Basin, offshore Vietnam, driven by climate change and tectonics, established from sequence biostratigraphy: Palaeogeography, Palaeoclimatology, Palaeoecology, v. 530, p. 113-135.

Phuong, K. L, 2014, Generation of authigenic clay minerals during diagenesis of Oligocene sandstone: Science & Technology Development, v.17, p.21-26.

Phuong, L. K, 2017, Characterization of petrography and diagenetic processes influence on porosity and permeability of Oligocene sandstone reservoir rocks, block 15-2 in Cuu Long basin: International Journal of Engineering Research and Applications, v. 07, p. 62-73.

Schmidt, W. J., B. H. Hoang, J. W. Handschy, V. T. Hai, T. X. Cuong, and N. T. Tung, 2019, Tectonic evolution and regional setting of the Cuu Long Basin, Vietnam: Tectonophysics, v. 757, p. 36-57.